IOP PUBLISHING NANOTECHNOLOGY
Nanotechnology **18** (2007) 145604 (5pp) doi:10.1088/0957-4484/18/14/145604

Mechanical and magnetic properties of Ni-doped metallic $TaSi_2$ nanowires

Yu-Lun Chueh[1,2], Li-Jen Chou[1], Jinhui Song[2] and Zhong Lin Wang[2]

[1] Department of Materials Science and Engineering, National Tsing Hua University, Hsinchu, Taiwan 300, Republic of China
[2] School of Materials Science and Engineering, Georgia Institute of Technology, Atlanta, GA 30332-0245, USA

E-mail: ljchou@mx.nthu.edu.tw and zhong.wang@mse.gatch.edu

Received 20 November 2006, in final form 7 January 2007
Published 6 March 2007
Online at stacks.iop.org/Nano/18/145604

Abstract
Ni-doped $TaSi_2$ nanowires were synthesized by annealing $NiSi_2$ film as the mediated layer in a Ta reductive ambient at 950 °C for 16 h. The hysteresis loop has a hard magnetization axis and high remanence with a coercive force of 120 Oe when the applied magnetic field is perpendicular to the substrate (parallel to the nanowires) and the hysteresis loop has an easy magnetization axis and low remanence with a coercive force of about 95 Oe when the applied magnetic field is parallel to the substrate (perpendicular to the nanowires). The elastic modulus of the nanowires was measured to be 170–485 GPa.

1. Introduction

Nanoscale materials are of considerable interest because they can be applied in various fields such as biomedical-, sensing-, photovoltaics-, opto- and spin-electronics devices owing to their unique or largely improved electric, mechanical, and magnetic properties [1, 2]. However, for the purpose of interconnects, nanowires with high melting point and low resistance are indispensable. The best candidate is silicide nanowires that possess a high meting point, low resistivity, mechanical stability, no reaction with final metal, and can be easily integrated with Si-based technology [3]. On the other hand, the magnetic metallic nanowires have attracted much attention as spin-based and/or magnetism-based devices, with which the electrons can be confined in the radial dimension by applying the magnetic field at various directions due to the magnetic anisotropy induced by the geometrical effect [4]. Recently, the refractory silicide, $TaSi_2$, with Ni doping of 4–8 at.%, has been successfully synthesized via $NiSi_2$ as the mediated layer [5]. The doping of Ni atoms in $TaSi_2$ nanowires may result in a magnetic nature since $TaSi_2$ has diamagnetic properties [6]. In this paper, we first illustrate the electronic structure of the $TaSi_2$ NWs using the information provided by electron energy-loss spectroscopy (EELS). Then the mechanical and magnetic properties of the NWs will be investigated for illustrating their performance to serve as nanoscale interconnects.

2. Experimental details

Single-crystal (001) Si wafers (1–30 Ω cm) were cleaned by the standard cleaning process. A 30 nm thick film was deposited on Si substrate by an ultrahigh vacuum e-beam deposition system at room temperature. The as-deposited samples were annealed at 850 °C for 30 min without breaking the vacuum chamber to form the $NiSi_2$ film and nanodot samples on the Si substrate. As-annealed samples were transferred into a Ta filament heating chamber for annealing at a pressure of lower than 1×10^{-6} Torr at 850–950 °C for different periods of time. The Ta atoms were vaporized constantly as the supplementary source for the growth of nanowires [7]. A field-emission transmission electron microscope (TEM: JEM-3000F, operated at 300 kV with point-to-point resolution of 0.17 nm) equipped with an energy dispersion spectrometer (EDS) and electron energy loss spectroscopy (EELS) was used to obtain the information on the microstructures and the chemical compositions. All of the raw EELS spectra were calibrated in the relative energy position by a zero-loss peak, and then subtracted by a power law to remove the background signal generated by multiple-scattering events. After re-calibrating the energy position and removing the multiple-scattering effect, the EELS was deconvoluted by the plasmon and low loss spectrum via the Fourier-log method to obtain the true single-scattering spectrum. The surface morphology was examined with a field-emission

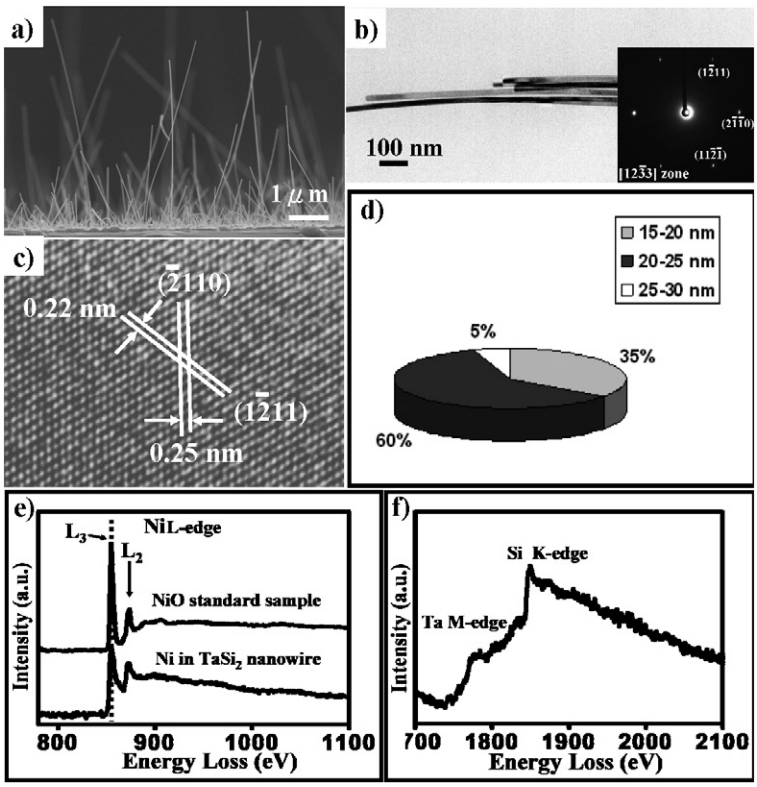

Figure 1. (a) The tilted SEM image of $TaSi_2$ nanowires (90° tilting). (b) The TEM image of these $TaSi_2$ nanowires. The inset shows the corresponding selected area electron diffraction pattern with the [12$\bar{3}\bar{3}$] zone axis recoded from a nanowire, indicting the growth direction along [2$\bar{1}\bar{1}$0]. (c) The corresponding high-resolution TEM image. (d) The statistic estimation of diameter for these $TaSi_2$ nanowires. (e) The EELS spectra of the Ni L edge for TaSi nanowire and NiO standard samples. (f) The EELS spectra for the Ta M edge and Si K edge.

scanning electron microscope (SEM: JSM-6500F), operated at 15 kV. The magnetic properties were characterized by a vibrating sample magnetometer (VSM) and superconducting quantum interference device (Quantum Design SQUID). The mechanical properties were carried out by and atomic force microscope (AFM) approach with the contact mode.

3. Results and discussions

The $TaSi_2$ nanowires (NWs) used in present study were synthesized by annealing the $NiSi_2$ film as the mediated layer in a Ta reductive ambient at 950 °C for 16 h, as shown in figure 1(a). The TEM image of the nanowires shown in figure 2(a) indicates the single-crystal nature of the NW. The corresponding electron diffraction pattern in the inset confirms the $TaSi_2$ phase with the zone axis [12$\bar{3}\bar{3}$]. The corresponding high-resolution TEM image, as shown in figure 1(c) also confirms that the growth direction of the NW is along [2$\bar{1}\bar{1}$0] (the *a*-axis). The details of the growth mechanisms for these $TaSi_2$ nanowires have been reported elsewhere [7]. In addition, the diameters are about 20–30 nm, as shown in figure 1(d). The atomic concentrations of Ta = 32%, Si = 64%, and Ni = 4% are calculated from the corresponding EDS spectrum. It is worth pointing out that the atomic concentration of Ni in $TaSi_2$ nanowires is about 4–8%; this is responsible for the magnetic property of the nanowire. In the TEM, the electronic structure of a single NW can be investigated by EELS. From the observed fine structures in the ionization edges, the electronic structure in the valence band can be qualitatively identified. The EELS spectrum shown in figure 1(e) reveals that the Ni atoms in the sublattice (interstitial sites) are of neutral atom type by determining the intensity ratio of the white line L_3/L_2 edges, which is smaller than that for the NiO standard sample, while there is no shift seen for the L_3 and L_2 edges located at 855 and 873 eV, respectively [8]. In addition, the Ta energy loss near edge fine structure (ELNES) for the Ta M edge and Si K edge are shown in figure 1(f), respectively.

The Ni atoms in $TaSi_2$ are likely to be responsible for the observed magnetic properties due to a spontaneous alignment of the d electron spins to reduce the exchange energy [9]. Figure 2(a) shows the room-temperature VSM hysteresis loop curve of Ni-doped $TaSi_2$ nanowires where the magnetic field is applied parallel and perpendicular to the substrate, respectively. All of the M–H data are presented after subtracting the contribution from the Si substrate. Note that the diamagnetic feature of bulk $TaSi_2$ may result in a shift of the hysteresis loop along the applied field axis [10]. But this phenomenon was not found in the present study, as shown in magnified image in the inset of figure 2(a), indicating that the influence of the diamagnetic feature by $TaSi_2$ plays a minor role. In order to clarify whether the magnetic property of $TaSi_2$ is originated from the Ni-doped $TaSi_2$ nanowires or not, the identical sample was measured for comparison after all of the Ni-doped $TaSi_2$ nanowires on substrate were totally removed, as shown in the inset of figure 2(b). The hysteresis loop still remains but the intensity of the VSM hysteresis

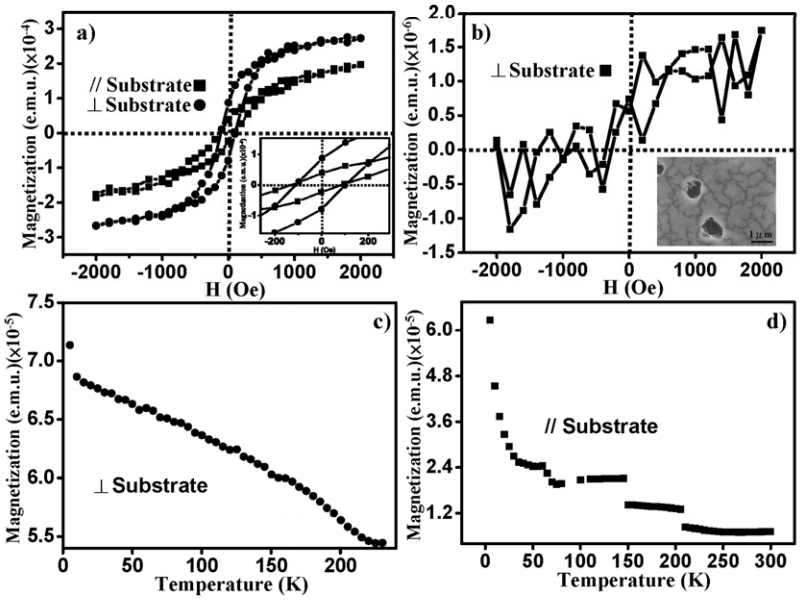

Figure 2. (a) VSM hysteresis loop curve of Ni-doped $TaSi_2$ nanowires at room temperature where the magnetic field is applied parallel and perpendicular to the substrate, respectively. The inset shows the magnified image taken from the zero field area. (b) The VSM hysteresis loop for the substrate after removing all the Ni-doped $TaSi_2$ nanowires. (c) and (d) The field-cooled (FC) measurements of the Ni-doped $TaSi_2$ nanowire perpendicular and parallel to the substrate measured by SQUID magnetometry.

loop is weak, with a significant shift away from the applied field axis, which is conjectured to be caused by diamagnetism of the $TaSi_2$ film on the substrate. The weak magnetic characteristic may be attributed to metal contamination or the $NiSi_2$ silicide layer [11]. Comparing the magnetization in the hysteresis loops presented in figures 2(a) and (b), it is clear that the magnetic properties have originated from the Ni-doped $TaSi_2$ nanowires. The hysteresis loop for the case of the applied magnetic field perpendicular to the substrate has a hard magnetization axis and high remanence (residual magnetization) with the coercive field of 120 Oe; meanwhile the hysteresis loop for the case of the applied magnetic field parallel to the substrate has an easy magnetization axis and low remanence (residual magnetization) with the coercive field of about 95 Oe. The high remanent and coercive fields may result from the shape anisotropy due to the quasi-vertical growth of $TaSi_2$ NW on the substrate, which forces the magnetic moments to mostly align along the axis of the nanowires. In addition, the defects inside the nanowire are another factor that can pin the domain. It needs greater applied field to break free. In general, the same saturation magnetization should be obtained by applying the magnetic fields perpendicular and parallel to the same sample if the size of the measured material is a bulk [12]. However, the saturated magnetization is different for the NWs when the magnetic field is perpendicular or parallel to the substrate. This is likely resulting from the non-identical magnetic coupling/interaction among the NWs due to their anisotropic aspect ratio. Figures 2(c) and (d) show the field-cooled (FC) measurements of the Ni-doped $TaSi_2$ nanowire by SQUID magnetometry. The FC measurement exhibits the behaviour of trapping the magnetic moment by anisotropic energy due to the fact that the magnetic moment is aligned along the direction of the applied magnetic field during the cooling process. For SQUID measurement, the sample is prepared as a rectangular shape with size of 3 mm × 5 mm, while for the VSM measurements, the samples are prepared in a square shape with sizes of 10 mm × 10 mm, resulting in a different scale of magnetization of the hysteresis loop and the FC measurements when the magnetic field is applied. From figures 2(c) and (d), it is apparent that both magnetizations decreased as the temperature was increased due to the thermal activation being large enough to reorient the magnetic moment to the orientation of the easy axis. The roughly linear dependence with temperature by applying the magnetic field perpendicular to the substrate, as shown in figure 2(c), seems to obey the Curie law, indicating a paramagnetic-like feature. It is well known that when the diameter of a materials is smaller than a critical value, a single magnetic domain is more suitable (e.g. ∼10 nm for Ni and Fe) [13]. Accordingly, the Ni atoms inside the $TaSi_2$ NW can be considered to be a lot of single magnetic domains due to the long length of the NWs. During the FC measurements, these single magnetic domains can be thermally agitated easily to prevent the existence of stable magnetization, whereas the pinning effect by defects inside the $TaSi_2$ NWs may have opposite results. This paramagnetic behaviour, namely the linear behaviour found in FC measurements in the present study, is considered to be balanced by the complementary compensation between size and pinning effects. The magnetization is found to be independent of the temperature when the magnetic field is applied parallel to the substrate (figure 2(d)). The tail found in figure 2(d) at low temperature is originated from the snapping off the domain wall pinned by defects under the applied magnetic field [14].

The elastic modulus of the NWs was measured by a technique developed by Song *et al* using an AFM in contact mode without destroying the sample [15]. A rectangular Si cantilever with a tetrahedral Si tip was used in present study,

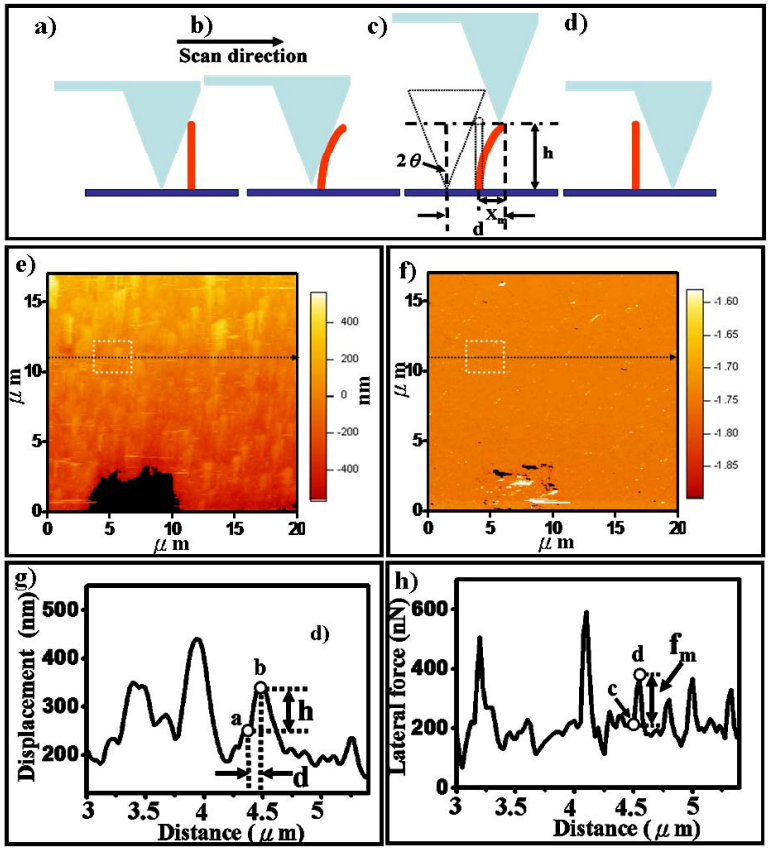

Figure 3. (a)–(d) The motion of a cantilever scan over the nanowires in an AFM in contact mode. (e) The topography image and (f) the lateral force image taken simultaneously from the AFM in contact mode. (g) Line profile of bending displacement as a function of scanning distance and (h) line profile of the lateral force as a function of the scanning distance recorded from the dashed line along the figures (e) and (f). h, d and f_m represent the largest bending height, scanning distance for the Si tip across the nanowires, and a constant lateral force when the scanner touches the nanowire.

(This figure is in colour only in the electronic version)

which had a calibrated normal spring constant of 1.8 N m^{-1} (AC240TS, Asylum Research). In addition, the lateral spring constant can be calculated from $KL = W_2 Kn/T_2$, where W and T represent the width and thickness of the cantilever and Kn means the normal force spring constant. The set point (constant normal force) and scanning speed are maintained at 100 nN and 7 μm s^{-1}, respectively. The overall behaviours of scanning over the nanowires in contact mode are schematically illustrated in figures 3 (a)–(d). The Si tip was in contact with the surface of the sample at a constant force (figure 3(a)). The motion of the scanning tip over the nanowires can be well controlled by surface morphology and lateral force. A small lateral force recorded by a photodetector was detected when the Si tip meets the nanowire (figure 3(b)). This lateral force was drastically increased as the Si tip consecutively scanned toward the nanowire so that the nanowire is elastically bent from its equilibrium position. At the largest bending position, the Si tip reaches the highest height and maximum lateral force (figure 3(c)). After the Si tip scan across the largest bending position, the nanowire was released, resulting in a sudden drop in the lateral force (figure 3(d)). Therefore, both the topography image (signal from the feedback of scanner) and lateral force image can be record simultaneously, as shown in figures 3(e) and (f) where the scanning area was set at 20 μm $\times$ 20 μm. Note that the bright tail in figure 3(e) results from the deflection along the scanning direction. The identical position in the lateral force image corresponding to the topography also shows a bright spot. In order to make sure that the centre of the tetrahedron can accurately meet the centre of the nanowires for theoretical calculation, the dashed line cross both same positions are made so that the displacement and lateral force as a function of the scanning distances can be found. Examples are shown in figures 3(g) and (h), which are derived from the dashed rectangle area of figures 3(e) and (f), respectively. From the displacement as a function of the scanning distance, as shown in figure 3(g), the d value in the x axis between points a and b means that the Si tip starts to touch the nanowires at the largest bending equilibrium position (figure 3(c)). The drop found behind the point b represents the Si tip crossing the nanowires. h represents the maximum bending height from the substrate. Subsequently, the elastic modulus for individual Ni-doped $TaSi_2$ nanowires can be estimated by taking the length of the nanowire, the average radius of the nanowire, and the lateral force spring constant [15], as given in table 1. The length of the nanowires and the corresponding elastic modulus ranged from 0.1355 to 0.3353 μm and 170 to 485 GPa, respectively. The average elastic modulus is approximately 302 GPa, which is consistent

Table 1. Length and elastic modulus of individual Ni-doped $TaSi_2$ nanowires measured with an AFM.

Nanowire	Length (μm)	Elastic modulus (GPa)
1	0.2336	343
2	0.2347	344
3	0.1355	172
4	0.3137	485
5	0.3352	390
6	0.2745	399
7	0.1456	258
8	0.3096	304
9	0.2443	207
10	0.1983	147
11	0.2974	396
12	0.1391	170
13	0.1449	312

with the value of 323 GPa for thin films (polycrystalline form) [16]. Note that the elastic modulus in the present study is increased as the length is increased. Similar phenomena are found for ZnO [17], and Ag [18] nanowires as well as carbon nanotubes (CNTs) [19] while some nanowires such as Cr [20] and Si [21] exhibit the opposite tendency. In addition, SiC [22] and Au [23] nanowires have no dependence on diameter. The details are still unknown and need to be investigated in the future. Comparing the elastic modulus with those of other nanowires by the electromechanical resonance method and atomic force microscopy method, such as carbon nanotube (1.28–0.6 TPa) [22], SiC (610–660 GPa) [22], ZnO (29–230 GPa) [15, 17], GaN (227–305 GPa) [24], and Si nanowires (93–250 GPa) [25, 26], the metallic Ni-doped $TaSi_2$ NWs have good mechanical properties, which are promising for nanodevice application in the future.

4. Conclusions

In summary, $TaSi_2$ nanowires can be synthesized with $NiSi_2$ as the mediated layer in a Ta reductive ambient annealed at 950 °C for 32 h. The Ni atoms can be incorporated into the $TaSi_2$ nanowires during the growth with the concentration of 4–8%. The Ni-doped $TaSi_2$ nanowires show an interesting magnetic nature. The hysteresis loops on applying the magnetic field parallel and perpendicular to the substrate exhibit different behaviours, which likely resulted from shape anisotropy. On the other hand, the elastic modulus of these Ni-doped $TaSi_2$ nanowires, acquired by AFM measurement by simultaneously deriving the topography and lateral images in contact mode without ruining the sample, is consistent with the bulk value. These findings in the magnetic and mechanical properties are of importance for applications as nanodevices.

Acknowledgments

This research was supported by the National Science Council through Grant No. NSC 94-2215-E-007-019, the Thousand Horse Program No. 095-2917-1-007-014, NSF, the NASA Vehicle System Program, Department of Defense Research and Engineering (DDR&E), the Defense Advanced Research Project Agency (N66001-040-1-18903).

References

[1] Greytak A B, Barrelet C J, Li Y and Lieber C M 2005 *Appl. Phys. Lett.* **87** 151103
[2] Arnold M S, Avouris P, Pan Z W and Wang Z L 2003 *J. Phys. Chem.* B **107** 659
[3] Murarka S P 1980 *J. Vac. Sci. Technol.* **17** 775
[4] Zhang D, Liu Z, Han S, Li C, Lei B, Stewart M P, Tour J M and Zhou C 2004 *Nano Lett.* **4** 2151
[5] Chueh Y L, Ko M T, Chou L J, Chen L J, Wu C S and Chen C D 2006 *Nano Lett.* **6** 1637
[6] Gottlieb U, Sulpice A, Madar R and Laborde O 1993 *J. Phys.: Condens. Matter* **5** 8755
[7] Chueh Y L, Chou L J, Cheng S L and Tasi C J 2003 *Appl. Phys. Lett.* **81** 5048
[8] Leapman R D, Grunes L A and Fejes P L 1982 *Phys. Rev.* B **26** 614
[9] Kasap S O 2002 *Principle of Electronic Materials and Devices* 2nd edn (New York: McGraw-Hill)
[10] Kodama R H, Makhlouf S A and Berkowitz A E 1997 *Phys. Rev. Lett.* **79** 1393
[11] Jentzsch F, Schad R, Heun S and Henzler M 1991 *Phys. Rev.* B **44** 8984
[12] Ross C A *et al* 2002 *Phys. Rev.* B **65** 144417
[13] Fonsea F C, Goya G F, Jardim R F, Muccillo R, Carreño N L, Longo E and Leite E R 2002 *Phys. Rev.* B **66** 104406
[14] Jiu Y Z, Hsu W K, Chueh Y L, Chou L J, Zhu Y Q, Brigatti K, Kroto H W and Walton D R M 2004 *Angew. Chem. Int. Edn* **43** 5670
[15] Song J h, Wangm X D, Riedo E and Wang Z L 2005 *Nano Lett.* **5** 1954
[16] Sidorenko S I, Makogon Y N, Beke D L, Csik A, Dub S N, Pavlova E P and Zelenin O V 2003 *Power Metall. Met. Ceram.* **42** 14
[17] Chen C Q, Shi Y, Zhang Y S, Zhu J and Yan Y J 2006 *Phys. Rev. Lett.* **96** 075505
[18] Cuenot S, Fretigny C, Demoustier-Champagne S and Nysten B 2004 *Phys. Rev.* B **69** 165410
[19] Poncharel P, Wang Z L, Ugarte D and de Heer W A 1999 *Science* **283** 1513
[20] Nilsson S G, Borrise X and Montelius L 2004 *Appl. Phys. Lett.* **85** 3555
[21] Li X, Ono T, Wang Y and Esashi M 2003 *Appl. Phys. Lett.* **83** 3081
[22] Wong E W, Sheehan P E and Lieber C M 1997 *Science* **277** 1971
[23] Wu B, Heidelberg A and Boland J J 2005 *Nat. Mater.* **4** 525
[24] Nam C Y, Jaroenapibal P, Tham D, Luzzil D E, Evoy S and Fischer J E 2006 *Nano Lett.* **6** 153
[25] Tabib-Azar M, Nassirou M, Wang R, Sharma S, Kamins T L, Islam M S and Williams R S 2005 *Appl. Phys. Lett.* **87** 113102
[26] Hoffmann S, Utke I, Moser B, Michler J, Christiansen S H, Schmidt V, Senz S, Werner P, Gösele U and Ballit C 2006 *Nano Lett.* **6** 662